ELSEVIER

Atmospheric Research 62 (2002) 209–237

ATMOSPHERIC RESEARCH

www.elsevier.com/locate/atmos

Particle size dependent response of aerosol counters ☆

A. Ankilov [1], A. Baklanov [1], M. Colhoun [2], K.-H. Enderle [3], J. Gras [4], Yu. Julanov [5], D. Kaller [6], A. Lindner [7], A.A. Lushnikov [5], R. Mavliev [1], F. McGovern [2], T.C. O'Connor [2], J. Podzimek [8], O. Preining, G.P. Reischl, R. Rudolf [9], G.J. Sem [10], W.W. Szymanski, A.E. Vrtala [11], P.E. Wagner *, W. Winklmayr [7], V. Zagaynov [5]

Institut für Experimentalphysik, Universität Wien, Boltzmanngasse 5, A-1090 Vienna, Austria

Abstract

During an international workshop at the Institute for Experimental Physics of the University of Vienna, Austria, which was coordinated within the Committee on Nucleation and Atmospheric Aerosols (IAMAS-IUGG), 10 instruments for aerosol number concentration measurement were studied, covering a wide range of methods based on various different measuring principles. In order to investigate the detection limits of the instruments considered with respect to particle size, simultaneous number concentration measurements were performed for monodispersed aerosols with particle sizes ranging from 1.5 to 50 nm diameter and various compositions. The instruments considered show quite different response characteristics, apparently related to the different vapors used in the various counters to enlarge the particles to an optically detectable size. A strong dependence of the 50% cutoff diameter on the particle composition in correlation with the type of vapor used in the

☆ Coordinated within the Committee on Nucleation and Atmospheric Aerosols, International Commission on Clouds and Precipitation, IAMAS-IUGG.

* Corresponding author.

E-mail address: paul.wagner@univie.ac.at (P.E. Wagner).

[1] Institute of Chemical Kinetics and Combustion, Novosibirsk, Russia.

[2] University of Galway, Galway, Ireland.

[3] GIV GmbH, Breuberg, Germany.

[4] Institute of Natural Resources and Environment, Aspendale, Victoria, Australia.

[5] Karpov Institute of Physical Chemistry, Moscow, Russia.

[6] Formerly Filipovicova.

[7] Hauke GmbH, Gmunden, Austria.

[8] University of Missouri-Rolla, Rolla, MO, USA.

[9] Present address: Stölzle Oberglas AG., Wien, Austria.

[10] TSI Inc., St. Paul, MN, USA.

[11] Formerly Majerowicz.

PII: S0169-8095(02)00011-X

specific instrument was found. An enhanced detection efficiency for ultrafine hygroscopic sodium chloride aerosols was observed with water operated systems, an analogous trend was found for *n*-butanol operated systems with nonhygroscopic silver and tungsten oxide particles.

Keywords: Particle detection efficiency; Condensation nuclei counter; Optical particle counter; Electro mobility spectrometer; Diffusion battery; Intercomparison study

1. Introduction

In recent years, the possible role of the atmospheric aerosol in the evolution of the global climate has received great attention (see e.g., Blanchet, 1989; Koepke, 1992). Consequently, the formation and dynamics of atmospheric aerosols have been studied by many authors (e.g., Kulmala et al., 2000). However, the global database on atmospheric aerosols appears to be still quite incomplete and the present measuring network needs to be improved (Deepak and Vali, 1991).

The number concentration is one of the most frequently determined parameters used for characterization of atmospheric aerosols and is among the aerosol parameters to be measured at global stations, according to recent international recommendations (Global Atmosphere Watch, 1999). There are various methods based on a number of different measuring principles, by which, determination of aerosol number concentration can be performed. In connection with comparison and interpretation of the data gathered by the different instruments in use, their response with respect to particle size and particle composition is important.

In this study, we investigated the performance of various types of condensation particle counters as well as several other instruments based on different measurement principles. The work was performed during an international workshop at the Institute for Experimental Physics of the University of Vienna, which was coordinated within the Committee on Nucleation and Atmospheric Aerosols, ICCP-IUGG to contribute to a comprehensive standardization of aerosol number concentration measurement systems.

Ten different instruments were considered, including Pollak counters in use already for several decades, presently available commercial particle counters, as well as laboratory prototypes. Particularly, we investigated various types of adiabatic expansion condensation particle counters, flow diffusion condensation particle counters and turbulent mixing condensation particle counters. Electrostatic aerosol spectrometers and a Faraday cup electrometer were used to characterize the test aerosols, the latter to provide an absolute concentration standard independent of particle composition.

In order to determine the response characteristics of the instruments considered under well-defined reproducible conditions, test aerosols with specified properties and known particle compositions have been used. Hygroscopic as well as nonhygroscopic particles were used in order to investigate a possible dependence of the response of aerosol particle counters on composition and physicochemical properties of the aerosols.

In the next section, the measuring principles of the various aerosol concentration measuring instruments considered in the present study, are briefly reviewed. The following

section contains a description of the general experimental arrangement used in the investigation of the instrument response with respect to particle size and composition, including the aerosol generation systems used. Subsequently, the measurement results are presented in detail and a few conclusions are drawn.

2. Experimental procedure

For intercomparison of aerosol measurement instruments regarding their response to different particle sizes, it is required to use well-defined and stable test aerosols that are delivered with virtually unchanged properties to all the instruments compared. For the evaluation of the cutoff characteristics of instruments, rather small particle sizes have to be used. In the present study, particle diameters down to 1.5 nm were considered. These aerosols are generally undergoing quite rapid dynamic changes and would cause significant instabilities in an aerosol plenum volume. Therefore, a three-stage dilution system and a linear aerosol flow system, as described in Ankilov et al. (2002), have been used in the present study when simultaneously comparing a larger number of different instruments. This arrangement has the advantage that steady state conditions can be achieved even for comparatively unstable test aerosols. However, the stability of the test aerosol sampled from a flow system critically depends on the stability of the aerosol generation, classification and dilution system. Accordingly, the test aerosol generation system comprised of the different aerosol generators, the classification system and the dilution systems were operated under carefully controlled conditions. During each measurement series, the properties of the test aerosol were continuously monitored. In a few cases when comparing only two instruments at a time, they could be directly connected to the dilution system, avoiding unnecessary additional problems with the linear flow system.

A schematic diagram of the experimental arrangement is shown in Fig. 1. Several different methods and compounds were used to generate the primary test aerosol for the detection efficiency investigations.

Sodium chloride (NaCl) aerosol of particles in the size range from 15 to 50 nm diameter was produced by atomizing dilute aqueous solutions of NaCl by means of a Collison atomizer (TSI 3076) with subsequent dilution and diffusion drying, followed by a classification in an electrostatic aerosol classifier (TSI 3071), to obtain fairly narrow size distributions.

Sodium chloride (NaCl) and silver (Ag) aerosols with diameters below about 20 nm were produced by evaporation in a tube furnace with subsequent nucleation and condensation. A similar type aerosol generator is described by Scheibel and Porstendörfer (1983).

Tungsten oxide particles were generated by radiation heating of an oxidized tungsten coil up to 1000 °C, causing emission of a high concentration of tungsten oxide molecules from the coil surface. The nucleation/condensation products were used as the primary aerosol.

The output of the various primary aerosol generators was monitored prior and after each single experiment by an Electro Mobility Spectrometer (EMS-1) of the Vienna type VIE-07, consisting of an ^{241}AM alpha source for bipolar charging, a Vienna type DMA and a

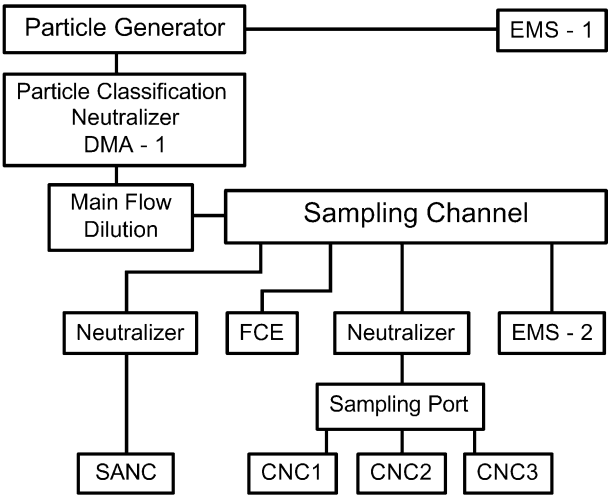

Fig. 1. Schematic diagram of the experimental arrangement showing the systems for aerosol generation, classification and dilution as well as the linear aerosol flow system and the various aerosol measurement instruments considered. The instruments used are listed in Table 1.

Vienna type Faraday cup electrometer (FCE) for concentration determination (Winklmayr et al., 1991).

Prior to introducing the aerosol into the main flow dilution system (described in detail in Ankilov et al., 2002), a monodispersed fraction was extracted by electrostatic classification. An ^{241}Am alpha source was used for bipolar charging and a Vienna Type DMA (DMA-1) for classification (Reischl et al., 1997).

The DMA ($R2 = 0.033$ m, $R1 = 0.025$ m and $L = 0.109$ m) was operated under symmetric flow conditions $Qsh = Qex = 25$ l/min. The flows were kept constant by means of critical orifices, as well as by a combination of precision pressure regulators in line with limiting orifices. With most of the generators used in this study delivering 2.5–5 l/min primary aerosol, the relative width of the extracted mobility fraction dZ/Z was in the range of 0.1–0.2, resulting in a relative standard deviation of the particle size distribution of 0.05–0.1.

For some of the experiments performed with only a small subset of different instruments, the aerosol flow rate through the classifier could be adjusted to smaller values to obtain narrower size distributions.

The monodispersed mobility fraction extracted from the classifier was introduced into the main dilution system without neutralisation. By this method, all the particles in the dilution system were unipolarly charged and the concentration was readily monitored by means of a FCE at any point of the system. However, aerosol neutralisation had to be applied prior to sampling from the main dilution system for each individual instrument or group of instruments.

Prior to all the experiments, an EMS (HAUKE EMS-08) was used to characterize the size distribution of the monodispersed test aerosol before the entrance into the main dilution system; for some experiments, a second Electro Mobility Spectrometer (EMS-2)

of similar type was used to monitor the diluted aerosol in the sampling channel during the entire experiment.

3. Instrumentation

In the present study, we considered 10 different instruments, which are based on three different measurement principles, for investigation of their response with respect to particle size and composition. In these instruments, measurement of aerosol number concentration is partly performed by single particle counting; in part, the concentration is determined from the measurement of an integral parameter. Some of these devices can be considered as absolute instruments, which are independent of empirical calibration relative to external reference standards. A few instruments, however, require empirical calibrations. While all of the measuring systems investigated provided data on particle number concentration, some of the instruments additionally allowed determination of aerosol size distribution. The latter instruments were used for characterization of the different test aerosols used.

The devices used and their measuring principles are listed in Table 1. The Pollak counters PCP, PCG and the Pollak type counter GIV CNC 440 are based on adiabatic expansion of initially water saturated aerosols causing vapor supersaturation and drop growth. The particle number concentration is determined from measurement of light extinction using an empirical calibration. A more detailed description of these instruments is given by Gras et al. (2002). The size analyzing nuclei counter (SANC 1) is based on adiabatic expansion as well, however, the number concentration of the growing droplets is determined from simultaneous light scattering and extinction measurements and quantitative comparison to Mie scattering theory. This method allows absolute number concentration measurement without calibration relative to an external standard (see Szymanski and Wagner, 1990; Szymanski, 2002).

The group of instruments TSI 3010, TSI 3022A and TSI 3025A are based on non-isothermal flow diffusion. Aerosols initially saturated with *n*-butanol vapor are passed in laminar flow through a cooled cylindrical tube and heat conduction leads to vapor supersaturation and drop growth. The concentration of the enlarged particles is determined either by optical single particle counting or, at higher concentrations, by an integral optical method requiring empirical calibration. A detailed description is given by Sem (2002).

The automated diffusion battery (ADB) and the diffusion aerosol spectrometer (DAS) are devices providing total particle number concentrations as well as aerosol size distributions. Prior to optical detection, the aerosol particles are magnified by condensation of supersaturated low volatility vapors of dibutyl phthalate (DBP), or dioctylsebacate. The supersaturation is achieved by the mixing of two gas flows at different temperatures. The aerosol number concentration is determined by counting the magnified particles. For details, see Julanov et al. (2002).

A somewhat similar principle is applied in the turbulent mixing type condensation nuclei counter (TM CNC) (Mavliev and Wang, 2000; Mavliev, 2002). Supersaturation of DBP vapor is obtained by turbulent mixing of a hot vapor-saturated particle-free flow with

Table 1
Aerosol measurement instruments used in the present study

Symbol	Acronym	Principle	Description	Institution
#	PCP	EXP	Pollak counter	University of Missouri-Rolla, MO, USA
×	PCG	EXP	Pollak counter	Institute of Natural Resources and Environment Aspendale, Victoria, Australia
■	GIV CNC-440	EXP	Pollak type counter Netzsch CNC-440	Netzsch Gerätebau, Germany GIV, Breuberg, Germany
●	SANC 1	EXP	Size analyzing nuclei counter	Institut für Experimentalphysik, Universität Wien
△	TSI 3010	DIFF	TSI condensation particle counter 3010	TSI, St. Paul, MN, USA
○	TSI 3022A	DIFF	TSI condensation particle counter 3022A	TSI, St. Paul, MN, USA
▽	TSI 3025A	DIFF	TSI ultrafine condensation particle counter 3025A	TSI, St. Paul, MN, USA
◇	ADB	MIX	Automated diffusion battery	Institute of Chemical Kinetics and Combustion, Novosibirsk, Russia
□	DAS	MIX	Diffusion aerosol spectrometer	Karpov Institute of Physical Chemistry, Moscow, Russia
Y	TM CNC	MIX	Turbulent mixing type condensation nuclei counter	Institute of Chemical Kinetics and Combustion, Novosibirsk, Russia
	HAUKE EMS-07	STAT	Electrical mobility spectrometer EMS-07	Hauke, Gmunden, Austria
	HAUKE EMS-08	STAT	Electrical mobility spectrometer EMS-08	Hauke, Gmunden, Austria
	FCE	STAT	Faraday cup electrometer FCE-07	Institut für Experimentalphysik, Universität Wien

Measuring principles of the instruments: EXP: adiabatic expansion condensation nuclei counter (working fluid: water); DIFF: flow diffusion condensation nuclei counter (working fluid: *n*-butanol); MIX: turbulent mixing condensation nuclei counter (working fluid: dibutyl phthalate); STAT: electrostatic particle measurement system.

a cold aerosol flow. Condensational growth of the aerosol particles to visible sizes allows number concentration determination by optical single particle counting.

The electrical mobility spectrometers HAUKE EMS-07 and HAUKE EMS-08 (see Reischl et al., 1997) allow the determination of particle number size distributions and have been used to monitor the test aerosols. Aerosol particles, which are brought into a bipolar electrical charge equilibrium by a neutralizer, are subsequently electrostatically classified. The concentrations of the thereby obtained series of aerosol mobility fractions are determined from measurements of electrical currents occurring in a Faraday cup electrometer. The number size distributions are calculated, accounting for the actual charging probabilities, and the total particle number concentration is obtained by integration over the entire size range.

The Faraday cup electrometer (FCE) is applicable only for measurement of the concentration of particles carrying unipolar electrical charges. Since the test aerosols used in this study were obtained by electrostatic classification of different polydispersed primary aerosols, all the particles carried charges of one sign only. For sufficiently small

particle diameters, the influence of multiple charges on the particles is negligible and the particle number concentration can be directly obtained from the FCE current and the aerosol intake flow rate. For larger particle sizes, however, a correction for multiple charges has to be applied using additional information about the number size distribution of the aerosol sample. In this study, the number size distribution was obtained by a HAUKE EMS-08 electrical mobility spectrometer. Since the number concentration information obtained by the FCE is independent of particle size and particle composition, the FCE provides an absolute reference standard for the previously mentioned devices.

4. Results and discussion

4.1. NaCl: general intercomparison results (NaCl CUT 1)

Simultaneous investigations of the detection efficiency of most of the instruments considered were performed using the experimental setup described in Ankilov et al. (2002).

The primary aerosol was produced by the tube furnace generator, a monodispersed fraction was extracted by electrostatic classification. The geometric standard deviation of the monodispersed test aerosol was between 1.04 for the larger particles (20 nm) and 1.10 for the smallest particles extracted (2.5 nm). Typical number size distributions of the test aerosol measured by the HAUKE EMS-VIE-08 (EMS-2) are shown in Fig. 2a–c.

For the general comparison (NaCl CUT 1), the overall results are presented in Fig. 3. The relative particle concentration plotted versus the particle diameter is obtained for each instrument by using the respective concentration obtained from the FCE as the standard, since the reading from an FCE is particle size independent and corrections for multiple charges (calculated from the measured size distributions) have been found to be negligible.

As expected, the TSI 3025A ultrafine condensation particle counter (reversed open triangles) reveals the highest counting efficiency over the whole size range closely followed by the Turbulent Mixing Type CNC (TM CNC, symbol Y) with a 50% cutoff diameter around 3 nm. Only slightly less efficient, the PCG Pollak CNC shows a 50% cutoff of about 3.5 nm. A rather large group of instruments (the GIV NETZSCH CNC-440, the SANC I, the TSI 3022A and the automated diffusion battery (ADB)) show distinctly larger 50% cutoff diameters between 5 and 7 nm. A 50% cutoff diameter, somewhat larger than 10 nm, shows only the diffusion aerosol spectrometer (DAS) and the TSI 3010 condensation particle counter.

In Fig. 3a, a direct comparison of the PCG Pollak CNC with the TSI 3025A ultrafine condensation particle counter is shown. It has to be noted that the PCG uses water as condensing substance where the NaCl particles might grow easier in comparison to the *n*-butanol operated TSI 3025A.

In Fig. 3b, two water-operated instruments, the NETZSCH CNC-440 and the SANC I, are compared. Both instruments show quite similar behaviour.

Fig. 3c shows a direct comparison of all the instruments of the Turbulent Mixing CNC type that use particle magnification with dibutyl phtalate (DBP) as condensing substance, TM CNC, the ADB and the DAS. The great variety in the detection effi-

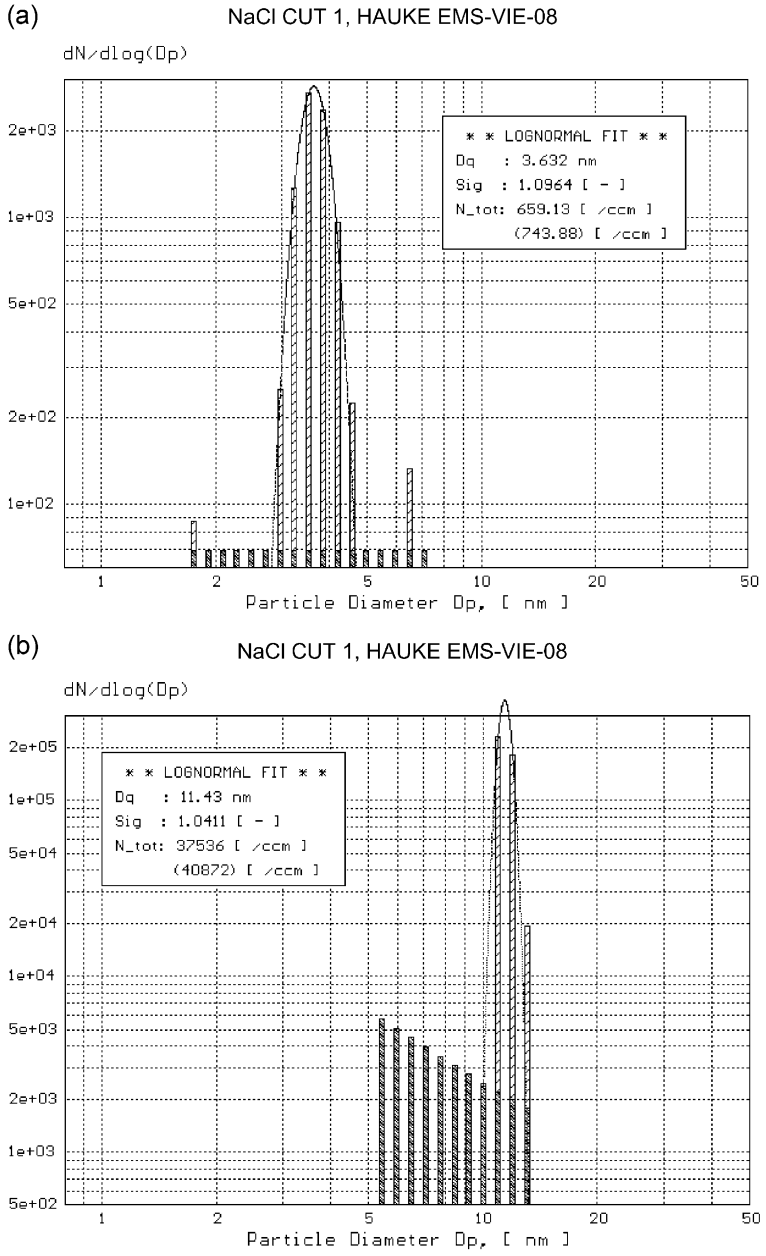

Fig. 2. Sample size distributions of monodispersed NaCl test aerosol, geometric mean particle diameter of 3.6 nm (a), 11.4 nm (b) and 18.5 nm (c), as measured by means of the HAUKE EMS-08.

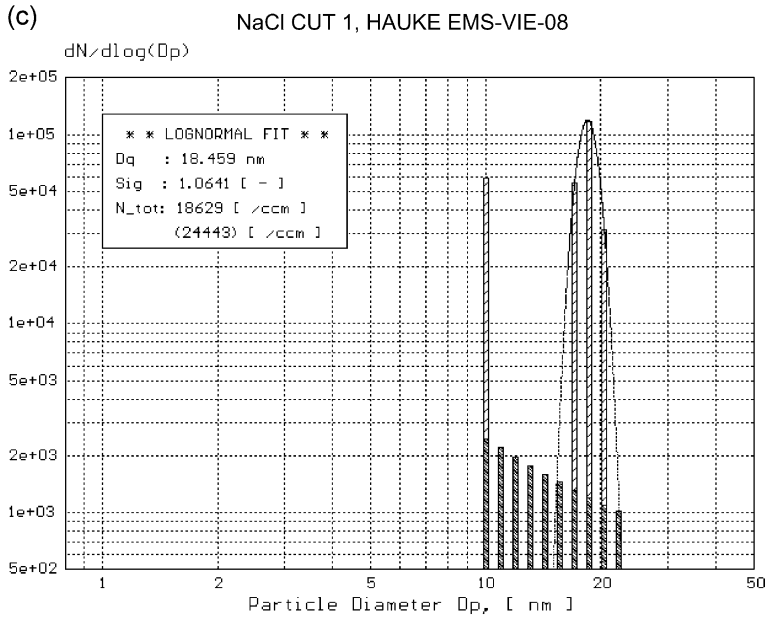

Fig. 2 (*continued*).

ciency might be explained by the different supersaturation levels applied in the individual instruments.

4.2. NaCl: intercomparison of a subset of instruments (NaCl CUT 2–CUT 4)

4.2.1. NaCl CUT 2

An additional experiment was performed to evaluate the performance of the TM CNC. For this purpose, the particle magnifier of the TM CNC was adjusted to the highest possible supersaturation level (close to the critical supersaturation of DBP where homogeneous nucleation is expected to occur). Fig. 4 shows a comparison of the optimally adjusted TM CNC with the TSI 3025A. The concentration values obtained from the Faraday cup electrometer were taken as the standard. As expected, the 50% cutoff diameter of the readjusted TM CNC is found to be shifted towards smaller particle diameters compared to the performance in experiment NaCl CUT 1 and can be located around 2.5 nm.

4.2.2. NaCl CUT 3

A similar experiment was performed to evaluate the performance of the automated diffusion battery (ADB). As in the previously described experiment, the particle magnifier of the ADB was adjusted to the highest possible supersaturation level. The concentration readings were compared with the results obtained from the FCE, the latter taken as the standard concentration determining device. Fig. 5 shows the resulting relative efficiency. The 50% cutoff diameter is found to be located around 2 nm, distinctly shifted towards smaller diameters compared to the performance in experiment NaCl CUT 1.

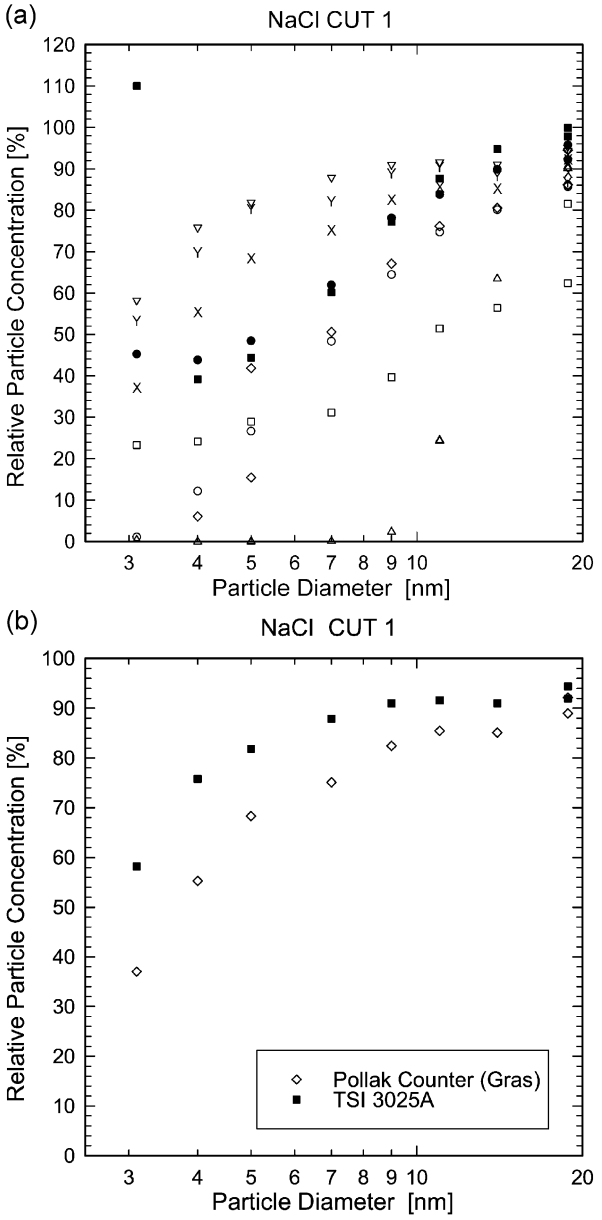

Fig. 3. Experiment NaCl CUT 1: response characteristics of all participating instruments for monodispersed NACl test aerosols, geometric mean particle diameters between 3 and 20 nm (a), comparison of the performance of subsets of instruments, PCG and TSI 3025A (b), GIV NETSCH-440 and SANC I (c) and the dibutyl phtalate operated instruments TM CNC, ADB and DAS (d).

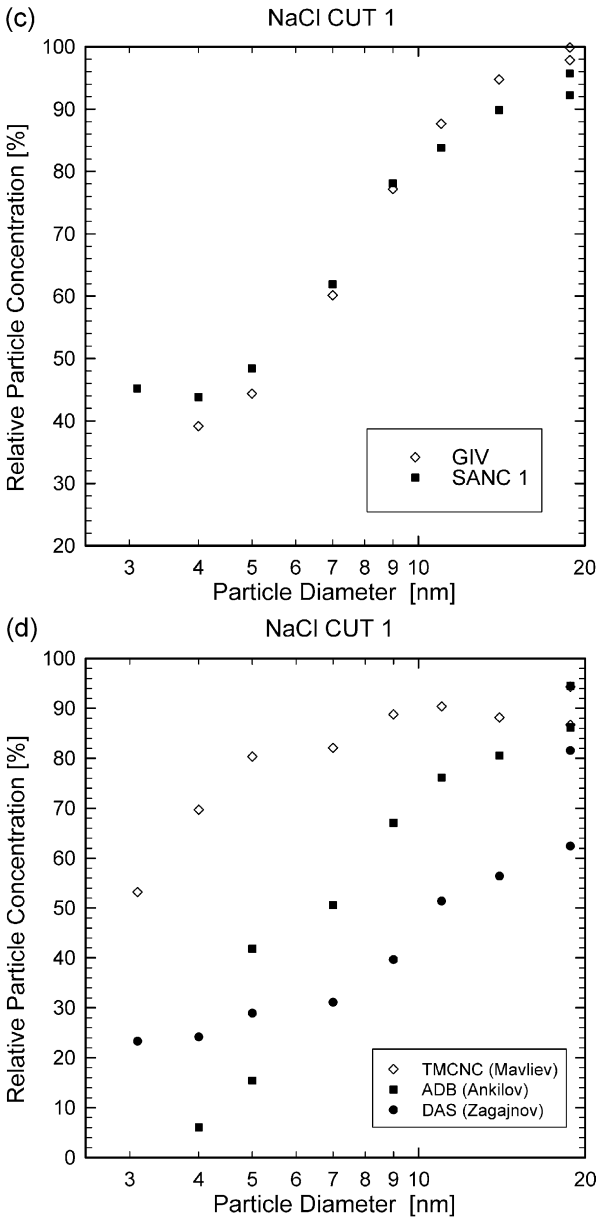

Fig. 3 (*continued*).

4.2.3. NaCl CUT 4

The detection efficiency of a subset of *n*-butanol operated CNCs, the TSI 3010, the TSI 3022A and the MET-ONE-1100, together with the water operated SANC 1 was investigated in a separate experiment (NaCl CUT 4).

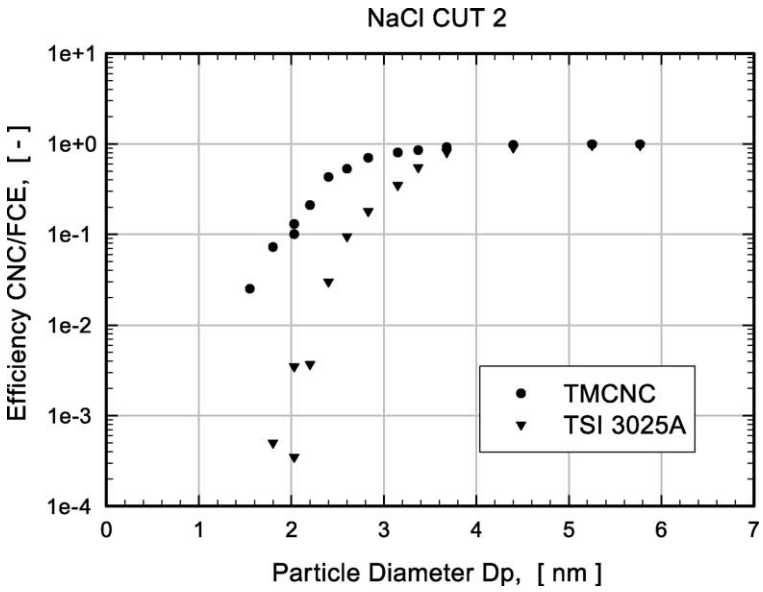

Fig. 4. Experiment NaCl CUT 2: response characteristics of the readjusted TM CNC and the TSI 3025A for monodispersed NACl test aerosols, geometric mean particle diameters between 1.5 and 6 nm.

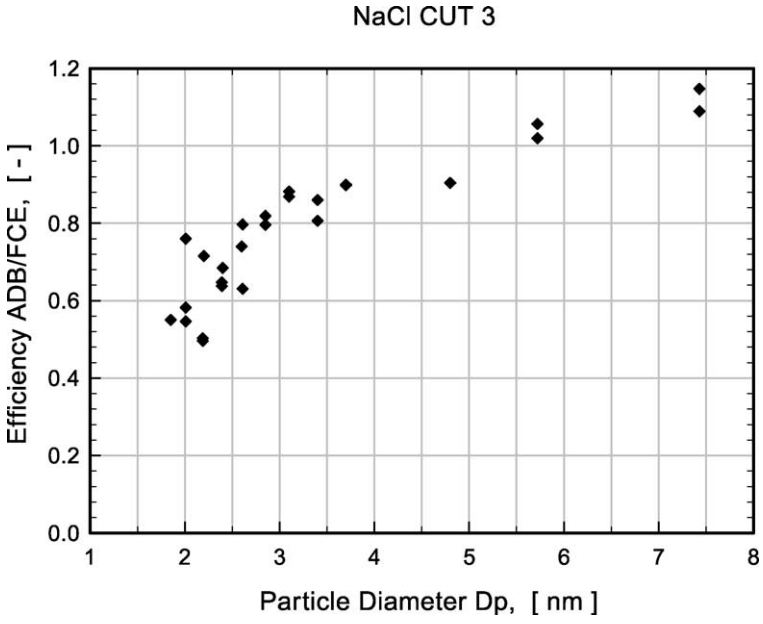

Fig. 5. Experiment NaCl CUT 3: response characteristics of the readjusted automated diffusion battery (ADB) for monodispersed NACl test aerosols, geometric mean particle diameters between 1.8 and 8 nm.

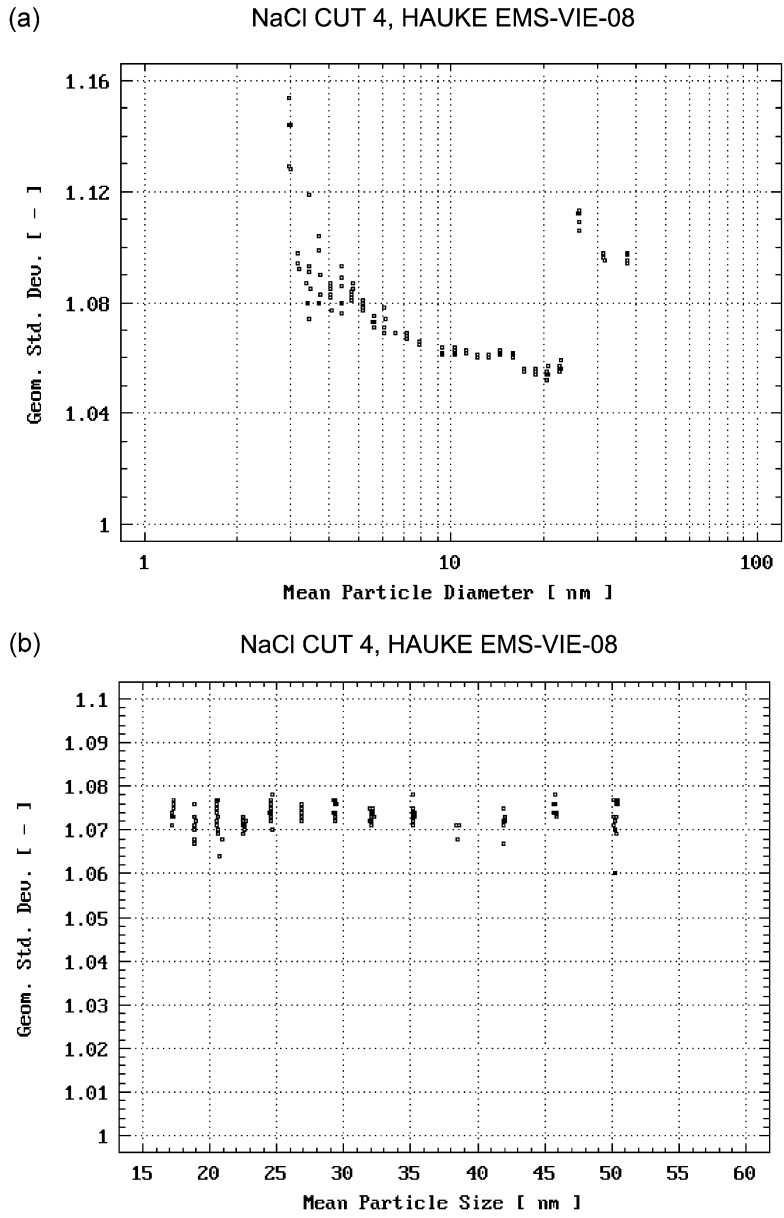

Fig. 6. Geometric standard deviations of NaCl test aerosols for the size range 3–20 nm (tube furnace generator with subsequent electrostatic classification) (a) and for 18–50 nm (collison atomizer with subsequent electrostatic classification) (b) used in experiment NaCl CUT 4.

This experiment had to be performed in subsequent steps using two different aerosol generators. For larger ultrafine particles in the size range between 17 and 50 nm, a Collison atomizer was used to generate the primary aerosol by atomizing a dilute solution of NaCl in ultrapure water. After diffusion drying and classification of the primary aerosol by the TSI 3071 Electrostatic Aerosol Classifier, the monodispersed test aerosol was characterized with the HAUKE EMS-VIE-08 and was found to have a geometric standard deviation of 1.07 over the entire size range (Fig. 6a). To obtain accurate reference concentrations from the FCE readings, the appropriate corrections for multiple charged particles were calculated from the number size distributions measured by the HAUKE EMS-VIE-08.

The tube furnace generator was used to generate the primary aerosol for the particle size range between 2.5 and 20 nm. The subsequent aerosol classification resulted in a fairly monodispersed aerosol with a geometric standard deviation of 1.05 for 20 nm geometric mean diameter up to 1.15 at 2.5 nm geometric mean diameter (Fig. 6b).

The 50% cutoff diameters for the *n*-butanol operated instruments are found to be significantly larger than for the water operated SANC I (Fig. 7). For the TSI 3010, a 50% cutoff diameter of 12.5 nm, for the TSI 3022A, a 50% cutoff diameter of 8 nm and for the MET-ONE-1100 a diameter of about 9 nm can be observed, the cutoff characteristics of the TSI 3010 and the MET-ONE-1100 being somewhat steeper than those of the TSI 3022A and the SANC I. However, for the MET-ONE-1100, some insecurities in the performance at larger particle sizes make a smaller value for the cutoff diameter more likely.

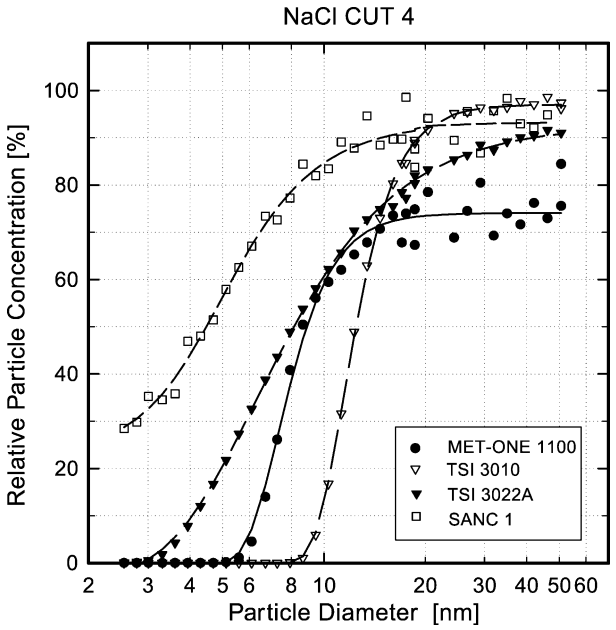

Fig. 7. Experiment NaCl CUT 4: response characteristics of a subset of instruments (MET ONE-1100, TSI 3010, TSI 3022A and SANC I) for monodispersed NaCl test aerosols, geometric mean particle diameters between 2.5 and 50 nm.

The observed enhanced counting efficiency of the SANC I (the only water operated instrument in this group) at small particle diameters with a 50% cutoff diameter of 4.5 nm might be due to the fact that NaCl is soluble in water.

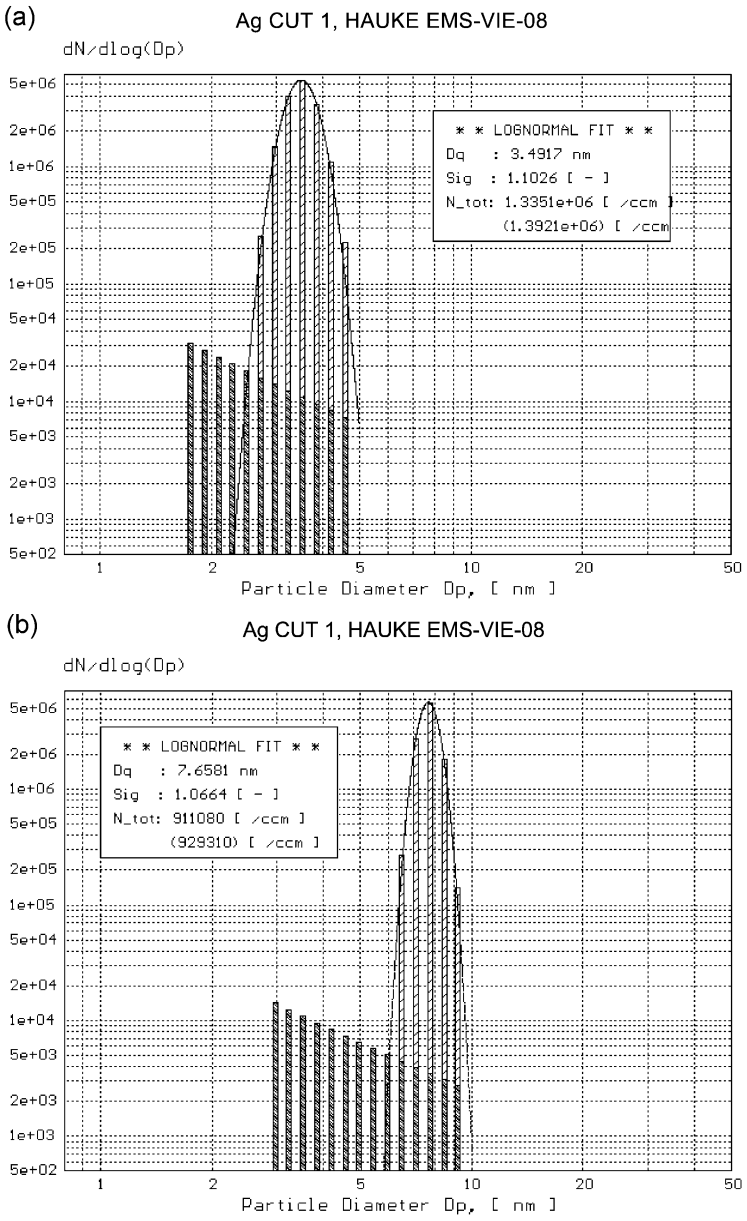

Fig. 8. Sample size distributions of monodispersed Ag test aerosols, geometric mean particle diameter of 3.5 nm (a), 7.7 nm (b) and 13.9 nm (c), as measured by means of the HAUKE EMS-08.

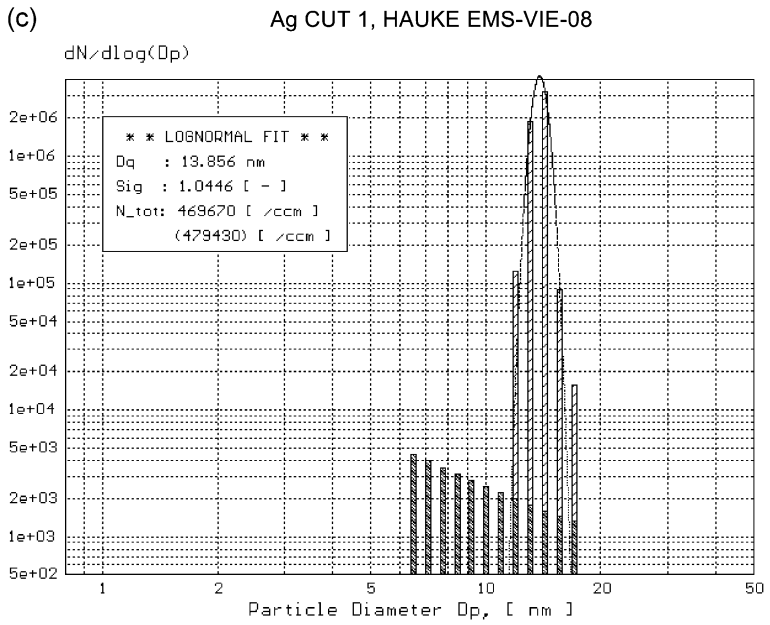

Fig. 8 (*continued*).

4.3. Silver: general intercomparison results (Ag CUT 1)

As for NaCl, the primary aerosol was produced by a tube furnace and a monodispersed fraction was extracted by electrostatic classification. However, the largest particle size that could be generated by this system was about 18 nm, limiting the range of instruments to be investigated more extensively. Using the HAUKE EMS-VIE-08 for characterization, the geometric standard deviation of the monodispersed test aerosol was found to be between 1.04 for the larger particles (14 nm) and 1.10 for the smallest particles extracted (2.5 nm) (see Fig. 8a–c).

The results of the general comparison (Ag CUT 1) are shown in Fig. 9. The relative particle concentration plotted versus the particle diameter is obtained for each instrument by using the respective concentration obtained from the FCE as the standard, since the reading from an FCE is particle size independent and corrections for multiple charges (calculated from the measured size distributions) have been found to be negligible throughout the considered size range.

The data obtained in this comparison experiment show quite remarkable scatter, some of the results from individual instruments seem to be inconsistent with the experiments using NaCl aerosol. Among the appealingly more reliable data, the TSI 3025A ultrafine condensation particle counter (reversed open triangles) reveals the highest counting efficiency over the whole size range closely followed by the Turbulent Mixing Type CNC (TM CNC, symbol Y) with a 50% cutoff diameter smaller than 3 nm. Somewhat less efficient, the PCG Pollak CNC and the SANC I shows a 50% cuttoff of about 4 nm. A

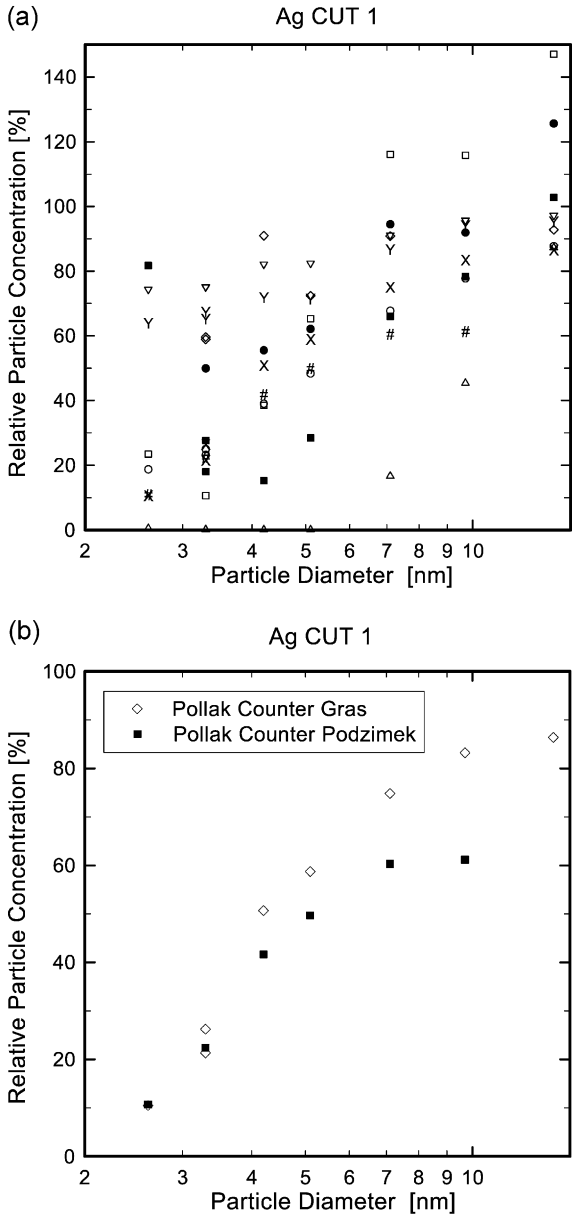

Fig. 9. Experiment Ag CUT 1: response characteristics of all participating instruments for monodispersed Ag test aerosols, geometric mean particle diameters between 2.5 and 20 nm (a), comparison of the performance of subsets of instruments, PCG and PCP (b) and the dibutyl phtalate operated instruments TM CNC, ADB and DAS (c).

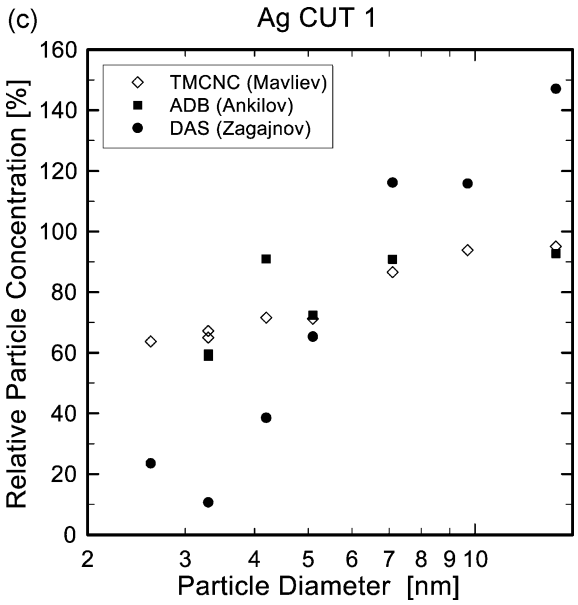

Fig. 9 (*continued*).

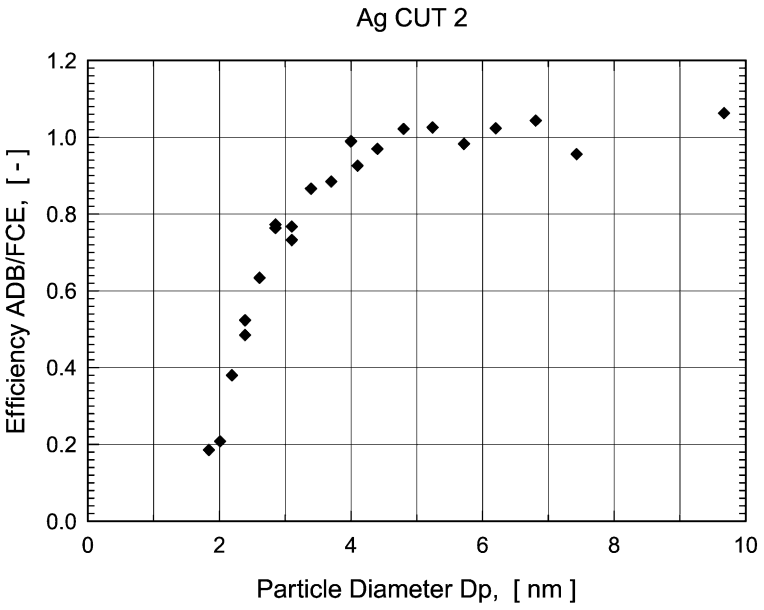

Fig. 10. Experiment Ag CUT 2: response characteristics of the readjusted automated diffusion battery (ADB) for monodispersed NACl test aerosols, geometric mean particle diameters between 1.8 and 10 nm.

group of instruments (the GIV NETZSCH CNC-440, the TSI 3022A and the PCO Pollak CNC) show distinctly larger 50% cutoff diameters between 5 and 7 nm. A 50% cutoff diameter, somewhat larger than 10 nm, are only found for the TSI 3010 condensation particle counter. The diffusion aerosol spectrometer (DAS) and the automated diffusion battery (ADB) show a much higher efficiency in this experiment compared to their performance in the experiment NaCl CUT 1, apparently due to the readjustment of the instruments. It is noticeable that the counting efficiency of the TM CNC and the TSI 3025A both show a very flat characteristic.

It can be further seen that both water operated instruments, the GIV NETSCH CNC-440 and the SANC I, have a somewhat larger 50% cutoff diameter for Ag compared to NaCl, whereas, e.g., the *n*-butanol operated TSI 3010 shows a somewhat smaller cutoff diameter for Ag compared to NaCl.

A direct comparison of the two Pollak counters participating in this experiment, the PCO and the PCP, reveal an apparent calibration problem of the PCP (Fig. 9a), However, the overall performance is quite comparable. For Ag aerosol, no apparent shift of the 50% cutoff diameter to larger values can be detected (as might be expected from the performance of the GIV NETSCH CNC-440 and the SANC I), although this group of instruments is water operated as well.

Fig. 9b shows a direct comparison of all the instruments of the type Turbulent Mixing CNC that use particle magnification with dibutyl phtalate (DBP) as condensing substance,

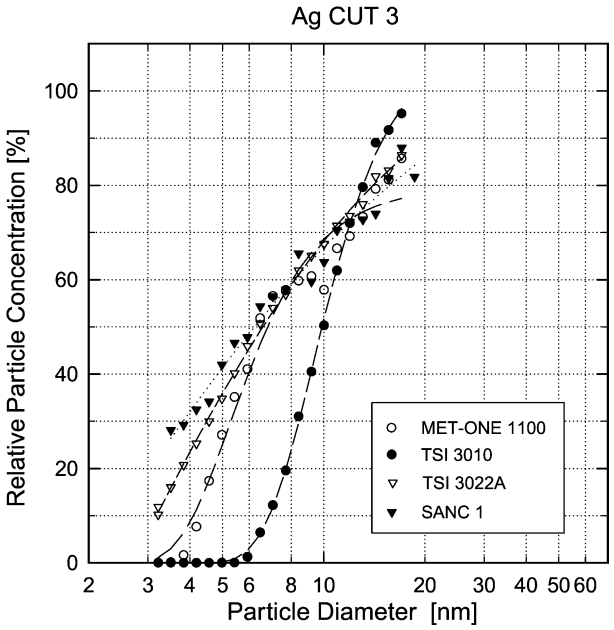

Fig. 11. Experiment Ag CUT 3: response characteristics of a subset of instruments (MET ONE-1100, TSI 3010, TSI 3022A and SANC I) for monodispersed Ag test aerosols, geometric mean particle diameters between 3 and 20 nm.

TM CNC, the ADB and the DAS. Although the large scatter of the data does not allow more detailed interpretations, some general remarks can be made. After readjustment of the instruments, the differences in the detection efficiencies between the three instruments

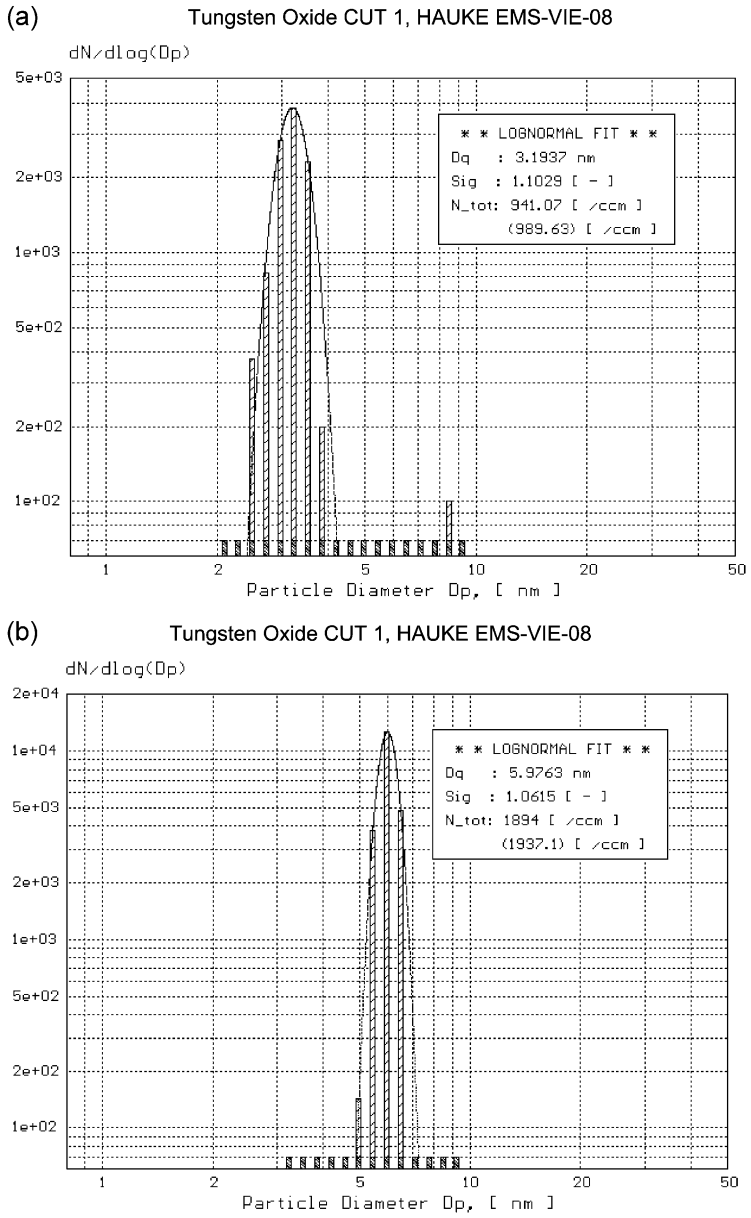

Fig. 12. Sample size distributions of monodispersed tungsten oxide test aerosols, geometric mean particle diameter of 3.2 nm (a), 6.0 nm (b) and 20.4 nm (c), as measured by means of the HAUKE EMS-08.

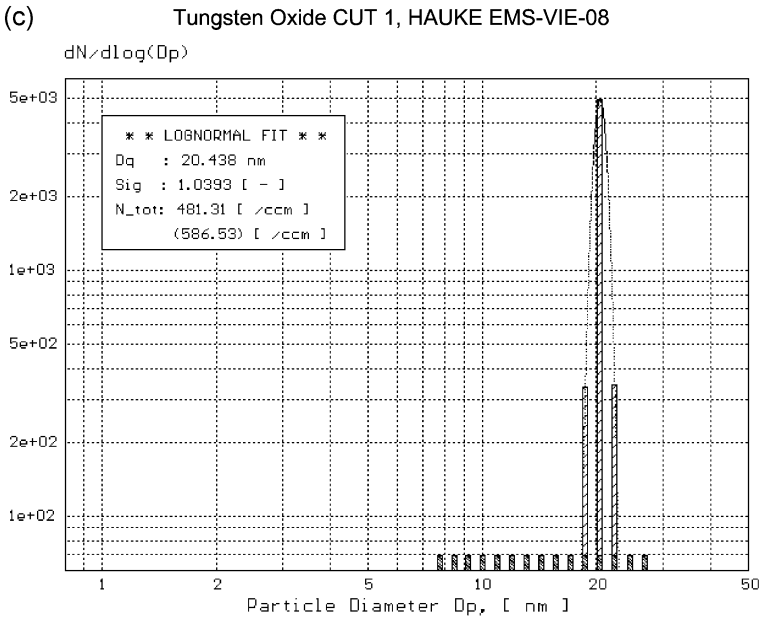

Fig. 12 (*continued*).

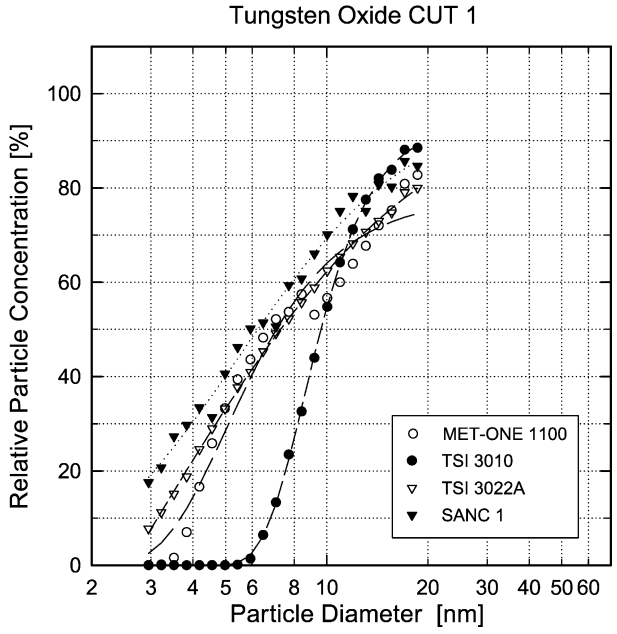

Fig. 13. Experiment Tungsten Oxide CUT 1: response characteristics of a subset of instruments (MET ONE-1100, TSI 3010, TSI 3022A and SANC I) for monodispersed tungsten oxide test aerosols, geometric mean particle diameters between 2.5 and 20 nm.

have become distinctively smaller compared to the performance in the experiment NaCl CUT 1. The TM CNC and the automated diffusion battery (ADB) reveal both a rather flat efficiency characteristic with quite comparable absolute values. The DAS shows a distinctly steeper characteristic of the counting efficiency in addition to an apparent calibration problem (overestimation of particle concentration).

4.4. Ag: intercomparison of a subset of instruments (Ag CUT 2–CUT 3)

4.4.1. Ag CUT 2

Because of some insecurity of the data obtained during the experiment Ag CUT 1 caused by slight interference with other instruments sampling from the linear flow system, an additional experiment was performed to evaluate the performance of the automated diffusion battery (ADB). The particle magnifier of the ADB was adjusted to the highest possible supersaturation level. The concentration readings were compared with the results obtained from the FCE, the latter taken as the standard concentration determining device. Fig. 10 shows the resulting relative efficiency. The 50% cutoff diameter is found to be located around 2.3 nm, somewhat shifted towards larger diameters compared to the performance in experiment NaCl CUT 3. It should be noted that the counting efficiency function for this instrument is extremely steep, it starts to drop below unity under 4-nm particle diameter.

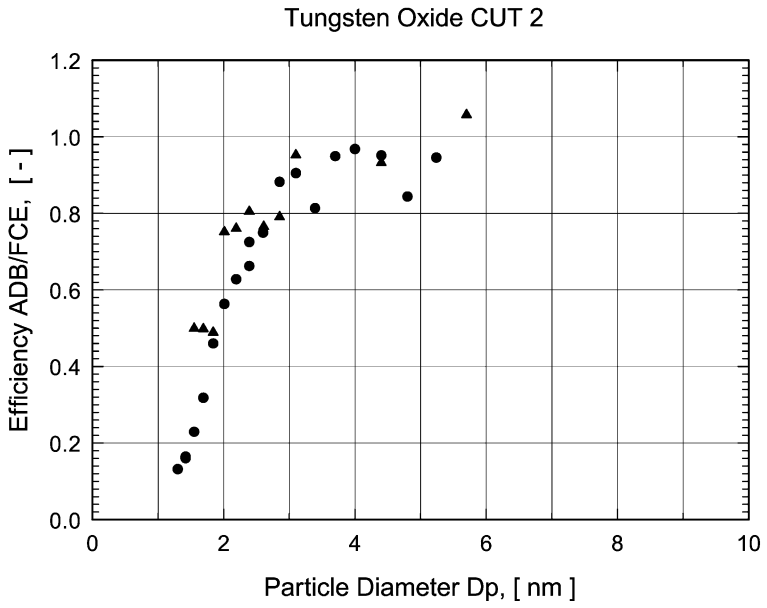

Fig. 14. Experiment Tungsten Oxide CUT 2: response characteristics of the readjusted automated diffusion battery (ADB) for monodispersed tungsten oxide test aerosols, geometric mean particle diameters between 1.5 and 6 nm.

4.4.2. Ag CUT 3

The detection efficiency of a subset of *n*-butanol operated CNCs, the TSI 3010, the TSI 3022A and the MET-ONE-1100, together with the water operated SANC 1 was investigated in a separate experiment (Ag CUT 3). Because of the lack of an aerosol generator able to generate particles larger than 20-nm mean diameter, only the size range below 20 nm could be investigated.

The tube furnace generator was used to generate the primary aerosol for the particle size range between 3 and 20 nm. The subsequent aerosol classification resulted in a fairly monodispersed aerosol with a geometric standard deviation of 1.05 for 20 nm geometric mean diameter up to 1.10 at 3 nm geometric mean diameter.

Unlike the performance of this group of instruments in the similar experiment with NaCl aerosol, for silver particles the 50% cutoff diameter for the comparable *n*-butanol operated instruments are found to be close to the 50% cutoff diameter for the water operated SANC I (Fig. 11). For the TSI 3022A, the MET-ONE-1100 and the SANC I a 50% cutoff diameter around 6.5 nm is observed. The cutoff characteristics of the MET-ONE-1100 appears to be somewhat steeper than those of the TSI 3022A and the SANC I, the latter showing the flattest one. For the TSI 3010, the steepest cutoff characteristic is observed. The respective 50% cutoff diameter of 10 nm is distinctly smaller for Ag aerosol than for NaCl. This trend can be observed for all *n*-butanol operated instruments in this group.

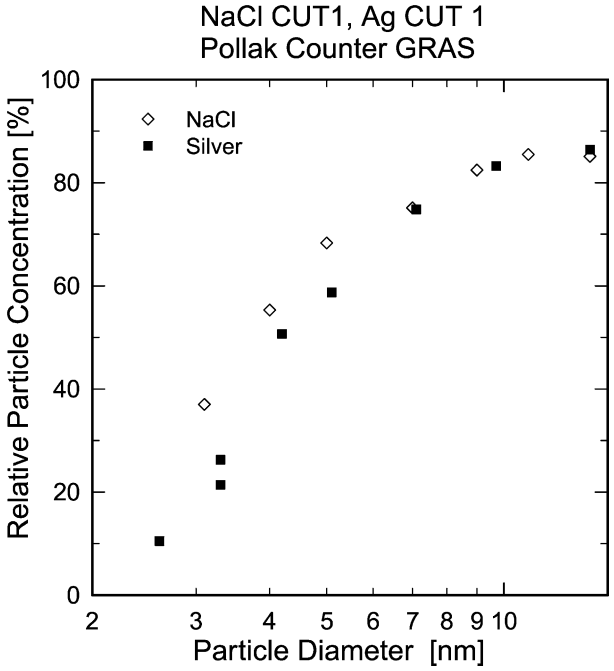

Fig. 15. Comparison of the response characteristics of the PCG Pollak counter with respect to NaCl and Ag test aerosols.

4.5. Tungsten oxide: intercomparison of a subset of instruments

4.5.1. Tungsten oxide CUT 1

The detection efficiency of a subset of *n*-butanol operated CNCs, the TSI 3010, the TSI 3022A and the MET-ONE-1100, together with the water operated SANC 1 was investigated for their performance using tungsten oxide aerosol. Because of the lack of an adequate aerosol generator able to generate particles larger than 20-nm mean diameter, only the size range below 20 nm could be investigated.

The primary aerosol of tungsten oxide particles was generated with the heated wire generator. The subsequent aerosol classification resulted in a fairly monodispersed aerosol with a geometric standard deviation of 1.05 for 20 nm geometric mean diameter up to 1.12 at 2.5 nm geometric mean diameter (Fig. 12a–c).

Similar to the performance of this group of instruments in experiment with Ag aerosol and also for tungsten oxide particles, the 50% cutoff diameter for the comparable *n*-butanol operated instruments are found to be close to the 50% cutoff diameter for the water operated SANC I (Fig. 13). For the TSI 3022A, the MET-ONE-1100 and the SANC I, a 50% cutoff diameter around 6.5 nm is observed. The cutoff characteristics of the MET-ONE-1100, the TSI 3022A and the SANC I are quite comparable, no significant qualitative differences can be detected. For the TSI 3010, a much steeper cutoff characteristic is observed. The respective 50% cutoff diameter of 10 nm is found to be the same for tungsten oxide aerosols as for Ag aerosols.

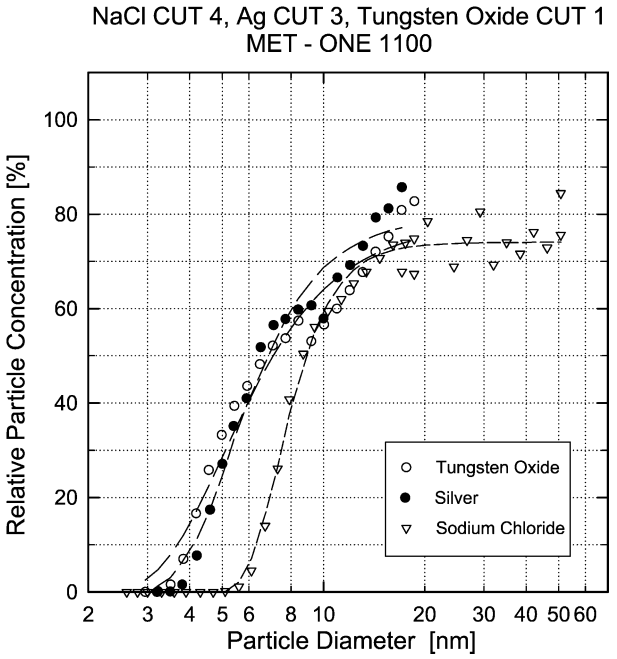

Fig. 16. Comparison of the response characteristics of the MET ONE-1100 condensation nucleus counter with respect to NaCl, Ag and tungsten oxide test aerosols.

4.5.2. Tungsten oxide CUT 2

An additional experiment was performed to evaluate the performance of the automated diffusion battery (ADB). The primary aerosol of tungsten oxide particles was generated with the heated wire generator running at very low heating currents to obtain smaller primary particles. At the subsequent aerosol classification, a higher sheeth airflow rate (56 l/min) was applied to the DMA, thereby decreasing the diffusion broadening of the transfer function for small particles. With this changed setup, monodispersed aerosol with geometric mean particle diameters from 1.5 up to 6 nm could be obtained. The respective geometric standard deviations were about 1.05 for 6-nm geometric mean diameter up to 1.25 at 1.5-nm geometric mean diameter.

The particle size magnifier of the ADB was adjusted to the highest possible supersaturation level. The concentration readings were compared with the results obtained from the FCE, the latter taken as the standard concentration determining device. Fig. 14 shows the resulting relative efficiency of two subsequent experiments (A and B). The 50% cutoff diameter is found to be located around 1.8 nm, somewhat shifted towards smaller diameters compared to the performance in experiment Ag CUT 2. Although the data for this experiment appear to be somewhat scattered and a minor calibration insecurity can be detected, the same steep characteristics of the efficiency function as for the other two aerosol substances (NaCl and Ag) can be observed, starting to drop below the reference level under 4 nm particle diameter.

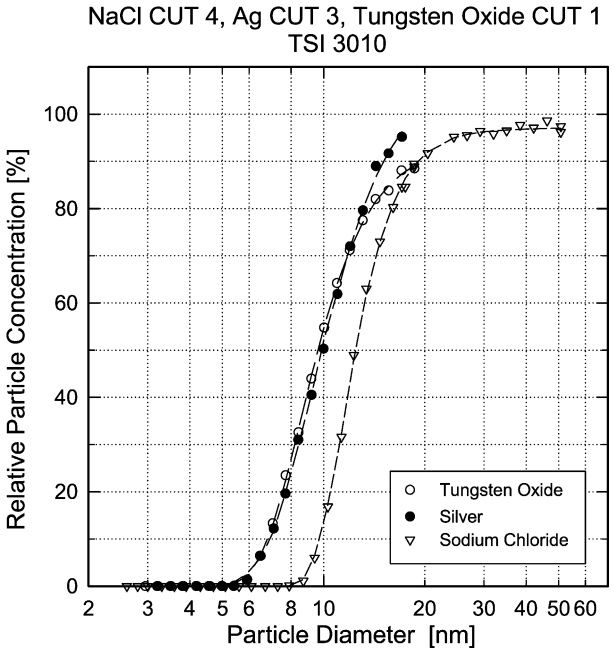

Fig. 17. Comparison of the response characteristics of the TSI 3010 condensation particle counter with respect to NaCl, Ag and tungsten oxide test aerosols.

5. Detection efficiency for different substances

The behaviour (detection efficiency) of selected instruments with respect to aerosol particle substance was evaluated using the data acquired during the experiments described in the previous sections.

Fig. 15 (NaCl CUT 1 and Ag CUT 1) shows a comparison of the performance of the PCO Pollak CNC with respect to Ag aerosol versus NaCl aerosol. It can be clearly seen that the detection efficiency of this water operated counter is significantly higher for the water-soluble NaCl particles than for Ag aerosol.

In Fig. 16, the data obtained for the MET ONE-1100 in the experiments NaCl CUT 4 (NaCl aerosol), Ag CUT 3 (silver aerosol) and Tungsten oxide CUT 1 (tungsten oxide aerosol) are plotted in one graph. Whereas the performance seems to be almost identical for Ag and tungsten oxide particles with a common 50% cutoff diameter of 6.5–7 nm and a quite comparable appearance of the detection efficiency function, a remarkable difference can be observed in the behaviour when sampling NaCl aerosol. The respective 50% cutoff diameter shifts to almost 9 nm and the detection efficiency function becomes noticeably steeper.

The same type of analysis was performed for the TSI 3010. Fig. 17 shows the data obtained for the instrument in the experiments NaCl CUT 4 (NaCl aerosol), Ag CUT 3 (silver aerosol) and Tungsten oxide CUT 1 (tungsten oxide aerosol) plotted in one graph. As for the MET ONE-1100, the two detection efficiency functions are almost identical for

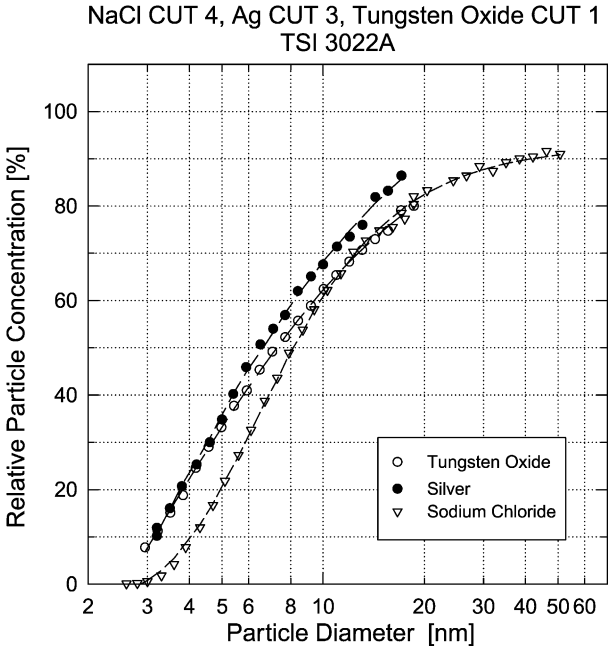

Fig. 18. Comparison of the response characteristics of the TSI 3022A condensation particle counter with respect to NaCl, Ag and tungsten oxide test aerosols.

Ag and tungsten oxide particles (with a minor difference for particles larger than 15-nm diameter), with a common 50% cutoff diameter of 10 nm. A similar remarkable difference can be observed for NaCl aerosol. The respective 50% cutoff diameter shifts to 12.5 nm and the detection efficiency function becomes noticeably steeper. (Note that the amount of shift of the 50% cutoff diameter is, for both instruments, about 25%).

For the TSI 3022A, this type of analysis reveals somewhat different results. Fig. 18 shows the data obtained for the instrument in the experiments NaCl CUT 4 (NaCl aerosol), Ag CUT 3 (silver aerosol) and Tungsten oxide CUT 1 (tungsten oxide aerosol) plotted in one graph. A similar remarkable difference as for the MET ONE-1100 and the TSI 3010 can be observed between the performance with NaCl aerosol and the performance with Ag aerosol. The respective 50% cutoff diameter shifts from 6.5 nm for Ag particles to 8.1 nm for NaCl particles (again a shift of about 25% in size), the detection efficiency function becomes somewhat steeper in the latter case. Unlike the two other *n*-butanol operated instruments (MET ONE-1100 and TSI 3010), the behaviour of the TSI 3022A with respect to tungsten oxide aerosol shows no unique tendency. For small particles (below 4 nm), the detection efficiency function runs close to the one obtained for Ag aerosol. For particle sizes above 10 nm, the behaviour seems to be close to that observed for NaCl aerosol, with a hybrid tendency in between. This results in a 50% cutoff diameter of about 7.3 nm for tungsten oxide particles.

For the water operated SANC I, this analysis shows the opposite trend compared to the two *n*-butanol operated instruments, MET ONE-1100 and TSI 3010. Fig. 19 shows the

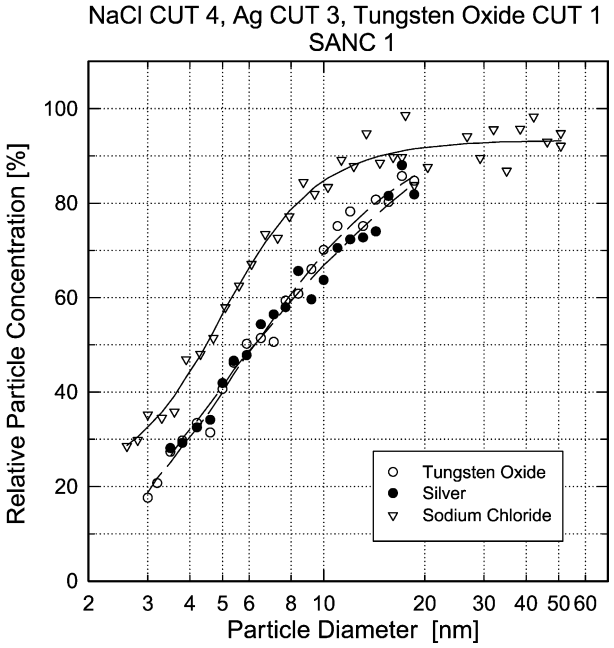

Fig. 19. Comparison of the response characteristics of the SANC I with respect to NaCl, Ag and tungsten oxide test aerosols.

data obtained for the SANC I in the experiments NaCl CUT 4 (NaCl aerosol), Ag CUT 3 (silver aerosol) and Tungsten oxide CUT 1 (tungsten oxide aerosol) plotted in one graph. As for the MET ONE-1100 and the TSI 3010, the detection efficiency functions are almost identical for Ag and tungsten oxide particles with a common 50% cutoff diameter of 6.3 nm. A remarkable difference with an opposite trend with respect to all of the *n*-butanol operated instruments can be observed for NaCl aerosol. The respective 50% cutoff diameter shifts to 4.5 nm (smaller particle sizes) and the detection efficiency function becomes noticeably steeper. The amount of shift of the 50% cutoff diameter is about −30%.

6. Conclusions

In joint experiments, we have investigated the particle size dependence of the response of several instruments measuring aerosol number concentrations. Some of the instruments considered were able to measure number size distributions by applying a size classifying method prior to concentration determination. Ten different instruments were considered, of which four were adiabatic expansion condensation particle counters, three were flow diffusion condensation particle counters and three were turbulent mixing condensation particle counters. Well-defined monodispersed test aerosols obtained by means of electrostatic classification of the primary aerosols, obtained from generators with three different particle compounds were applied. The polydispersed aerosols from the generators as well as the monodispersed test aerosols were continuously monitored by two Electro Mobility Spectrometers. A Faraday cup electrometer was used as an absolute reference standard for the aerosol concentration.

The response of the various instruments investigated depends strongly on the supersaturation of the vapor compound, causing heterogeneous condensation and particle growth to visible sizes as well as on the specific measuring technique applied. Consequently, quite different 50% cutoff diameters were observed for the different instruments. However, they were found to be quite well within the corresponding specifications.

Remarkable differences in the response of certain groups of instruments with respect to particle composition were observed. *n*-Butanol operated CNCs show a 25% shift of their 50% cutoff diameter towards larger particle sizes when sampling NaCl aerosol compared to the response with respect to silver aerosol. In contrast to that behaviour, the group of instruments that use water as condensing substance show an increased efficiency for small NaCl aerosol and consequently a shift of the 50% cutoff diameter up to 30% towards smaller particle diameters is observed, compared to the case when sampling silver aerosol. This effect might be due to the fact that NaCl is water soluble and not soluble in *n*-butanol (see Ankilov et al., 2002). For the dibutyl phtalate operated instruments, no conclusive results concerning their response with respect to particle composition could be obtained since the differences in the supersaturation adjustment in different experiments were causing some reproducibility problems. Except for one instrument, all the devices investigated show the same behaviour for tungsten oxide aerosol as for silver particles.

Finally, it should be emphasized that the differences in the 50% cutoff diameters of various instruments used for concentration determination as well as the dependence of

their response on particle composition is an important issue in connection with studies of nanoparticles and nucleation mode aerosols.

Acknowledgements

This work was supported by Universität Wien, Österreichische Akademie der Wissenschaften, Fonds zur Förderung der Wissenschaftlichen Forschung in Österreich, Gesellschaft für Aerosolforschung, Germany, TSI, USA, GIV, Germany, and Hauke, Austria.

References

Ankilov, A., Baklanov, A., Colhoun, M., Enderle, K.-H., Gras, J., Julanov, Yu., Kaller, D., Lindner, A., Lushnikov, A.A., Mavliev, R., McGovern, F., Mirme, A., O'Connor, T.C., Podzimek, J., Preining, O., Reischl, G.P., Rudolf, R., Sem, G.J., Szymanski, W.W., Tamm, E., Vrtala, A.E., Wagner, P.E., Winklmayr, W., Zagaynov, V., 2002. Intercomparison of number concentration measurements by various aerosol particle counters. Atmos. Res. 62, 177–207.

Blanchet, J.-P., 1989. Atmos. Environ. 23, 2609.

Deepak, A., Vali, G. (Eds.), 1991. The International Global Aerosol Program (IGAP) Plan. A. Deepak Publishing, Hampton, USA.

Global Atmosphere Watch, 1999. WMO GAW Information Sheet No. 15.

Gras, J.L., Podzimek, J., O'Connor, T.C., Enderle, K.-H., 2002. Nolan-pollak type CN counters in the Vienna aerosol workshop. Atmos. Res. 62, 239–354.

Julanov, Yu.V., Lushnikov, A.A., Zagaynov, V.A., 2002. Diffusion aerosol spectrometer. Atmos. Res. 62, 295–302.

Koepke, P., 1992. Nucleation and Atmospheric Aerosols. In: Fukuta, N., Wagner, P.E. (Eds.), A. Deepak Publishing, Hampton, USA, p. 485.

Kulmala, M., Pirjola, L., Mäkelä, J.M., 2000. Nature 404, 66.

Mavliev, R., 2002. Turbulent mixing condensation nucleus counter. Atmos. Res. 62, 303–314.

Mavliev, R., Wang, H.C., 2000. J. Aerosol Sci. 31, 933–944.

Reischl, G.P., Mäkelä, J.M., Necid, J., 1997. Aerosol Sci. Technol. 27, 651–672.

Sem, G.J., 2002. Design and performance characteristics of three continuous-flow condensation particle counters: a summary. Atmos. Res. 62, 267–294.

Scheibel, H.G., Porstendörfer, J., 1983. J. Aerosol Sci. 14, 113.

Szymanski, W.W., 2002. Aerosol concentration measurement with multiple light scattering system and laser aerosol spectrometer. Atmos. Res. 62, 255–265.

Szymanski, W.W., Wagner, P.E., 1990. J. Aerosol Sci. 21, 441–451.

Winklmayr, W., Reischl, G.P., Lindner, A.O., Berner, A., 1991. J. Aerosol Sci. 22, 289–296.